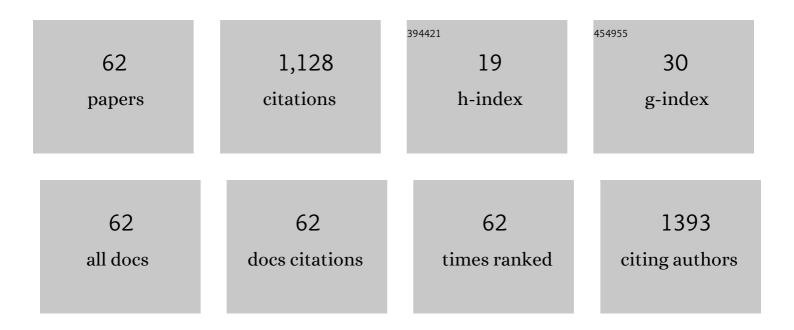
Feng Feng

List of Publications by Year in descending order

Source: https://exaly.com/author-pdf/2424714/publications.pdf Version: 2024-02-01



FENC FENC

#	Article	IF	CITATIONS
1	Facile synthesis of yellowish-green emitting carbon quantum dots and their applications for phoxim sensing and cellular imaging. Analytica Chimica Acta, 2022, 1206, 338685.	5.4	25
2	Ultralong lifetime room-temperature phosphorescence in aqueous medium from silica confined polymer carbon dots for autoluminescence-free bioimaging and multilevel information encryption. Dyes and Pigments, 2022, 197, 109890.	3.7	21
3	Durable room-temperature phosphorescence of nitrogen-doped carbon dots-silica composites for Fe3+ detection and anti-counterfeiting. Dyes and Pigments, 2022, 198, 109955.	3.7	13
4	A Low Cost Fe3O4–Activated Biochar Electrode Sensor by Resource Utilization of Excess Sludge for Detecting Tetrabromobisphenol A. Micromachines, 2022, 13, 115.	2.9	9
5	Tetracycline adsorption on magnetic sludge biochar: size effect of the Fe ₃ O ₄ nanoparticles. Royal Society Open Science, 2022, 9, 210805.	2.4	14
6	A novel ratiometric fluorescent probe for detection of l-glutamic acid based on dual-emission carbon dots. Talanta, 2022, 245, 123416.	5.5	17
7	Stimulus responsive luminescence and application of rotor type 1,1'-([2,2'-bithiophene]-3,3'-diyl)bis(ethan-1-one) and 3'-acetyl-[2,2'-bithiophene]-3-carbaldehyde as molecular rotors. Spectrochimica Acta - Part A: Molecular and Biomolecular Spectroscopy, 2022, , 121395.	3.9	0
8	A novel aptasensor based on HCR and G-quadruplex DNAzyme for fluorescence detection of Carcinoembryonic Antigen. Talanta, 2021, 221, 121451.	5.5	41
9	Intermetallic PdBi aerogels with improved catalytic performance for the degradation of organic pollutants in water. Chinese Chemical Letters, 2021, 32, 1451-1455.	9.0	13
10	Luminescence property of phosphoramidic acid oligomer nanodots in aqueous solution. Spectrochimica Acta - Part A: Molecular and Biomolecular Spectroscopy, 2021, 248, 119261.	3.9	4
11	A label-free fluorescent aptasensor based on HCR and G-quadruplex DNAzymes for the detection of prostate-specific antigen. Analyst, The, 2021, 146, 1340-1345.	3.5	14
12	The fluorescence imaging and precise suppression of bacterial infections in chronic wounds by porphyrin-based metal–organic framework nanorods. Journal of Materials Chemistry B, 2021, 9, 8048-8055.	5.8	10
13	Research Progress on the Synthesis of Covalent Organic Frameworks and Their Applications in Tumor Therapy. Acta Chimica Sinica, 2021, 79, 600.	1.4	8
14	Ternary Cocrystals with Large Soft Cavities: A 1,4â€diiodotetrafluorobenzene (DITFB)â‹4â€Biphenylpyridine N â€oxide (BPNO) Host Assembled by Inclusion of Planar Aromatic Guests. ChemPlusChem, 2021, 86, 252-258.	2.8	3
15	A label-free fluorescent sensor based on yellow-green emissive carbon quantum dots for ultrasensitive detection of congo red and cellular imaging. Microchemical Journal, 2021, 168, 106420.	4.5	12
16	Bidirectional modulation of microRNA with a clamp-like triplex switch for enhanced and programmed gene therapy. Chemical Communications, 2021, 57, 12131-12134.	4.1	0
17	Inhibition of noncanonical Wnt pathway overcomes enzalutamide resistance in castrationâ€resistant prostate cancer. Prostate, 2020, 80, 256-266.	2.3	22
18	Exploration of synthesizing fluorescent silicon nanoparticles and label-free detection of sulfadiazine sodium. Talanta, 2020, 220, 121410.	5.5	8

Feng Feng

#	Article	IF	CITATIONS
19	Synthesis of Stable Thiazole-Linked Covalent Organic Frameworks via a Multicomponent Reaction. Journal of the American Chemical Society, 2020, 142, 11131-11138.	13.7	158
20	Electrochemical Reduction-Assisted <i>In Situ</i> Fabrication of a Graphene/Au Nanoparticles@polyoxometalate Nanohybrid Film: High-Performance Electrochemical Detection for Uric Acid. Langmuir, 2020, 36, 7365-7374.	3.5	27
21	A label-free fluorescent sensor based on carbon quantum dots with enhanced sensitive for the determination of myricetin in real samples. Microchemical Journal, 2020, 157, 104956.	4.5	24
22	Human Serum Albumin-Occupying-Based Fluorescence Turn-On Analysis of Antiepileptic Drug Tiagabine Hydrochloride. Analytical Chemistry, 2020, 92, 3555-3562.	6.5	16
23	Self-supporting hierarchical PdCu aerogels for enhanced catalytic reduction of 4-nitrophenol. Journal of Hazardous Materials, 2020, 397, 122786.	12.4	35
24	Integrated Dual-Functional ORMOSIL Coatings with AgNPs@rGO Nanocomposite for Corrosion Resistance and Antifouling Applications. ACS Sustainable Chemistry and Engineering, 2020, 8, 6786-6797.	6.7	34
25	Inhibition of Rac1 reverses enzalutamide resistance in castration‑resistant prostate cancer. Oncology Letters, 2020, 20, 2997-3005.	1.8	10
26	Highly selective and sensitive detection of amaranth by using carbon dots-based nanosensor. RSC Advances, 2019, 9, 26315-26320.	3.6	25
27	Microwave rapid synthesis of CuxO@polypyrrole nanofibre (PpyNF) composites for supercapacitors. Fullerenes Nanotubes and Carbon Nanostructures, 2019, 27, 947-952.	2.1	3
28	Green synthesis of fluorescent carbon dots as an effective fluorescence probe for morin detection. Analytical Methods, 2019, 11, 353-358.	2.7	40
29	MIL/Aptamer as a Nanosensor Capable of Resisting Nonspecific Displacement for ATP Imaging in Living Cells. ACS Omega, 2019, 4, 9074-9080.	3.5	12
30	Real-Time Visualizing Mitophagy-Specific Viscosity Dynamic by Mitochondria-Anchored Molecular Rotor. Analytical Chemistry, 2019, 91, 8574-8581.	6.5	75
31	Inhibition of enhancer of zeste homolog 2 (EZH2) overcomes enzalutamide resistance in castration-resistant prostate cancer. Journal of Biological Chemistry, 2019, 294, 9911-9923.	3.4	66
32	Synchronous screening of multiplexed biomarkers of Alzheimer's disease by a length-encoded aerolysin nanopore-integrated triple-helix molecular switch. Chemical Communications, 2019, 55, 6433-6436.	4.1	19
33	Facile synthesis of polypyrrole nanofiber (PPyNF)/NiO _x composites by a microwave method and application in supercapacitors. RSC Advances, 2019, 9, 6890-6897.	3.6	28
34	Fluorescent boron and nitrogen co-doped carbon dots with high quantum yield for the detection of nimesulide and fluorescence staining. Spectrochimica Acta - Part A: Molecular and Biomolecular Spectroscopy, 2019, 216, 296-302.	3.9	23
35	Colorimetric and Ratiometric Fluorescence Dual-Mode Sensing of Glucose Based on Carbon Quantum Dots and Potential UV/Fluorescence of o-Diaminobenzene. Sensors, 2019, 19, 674.	3.8	20
36	Improved Efficiency of Perovskite Solar Cells by the Interfacial Modification of the Active Layer. Nanomaterials, 2019, 9, 204.	4.1	12

Feng Feng

#	Article	IF	CITATIONS
37	An improved class of fluorescent silica nanoparticles for indirect immunofluorescence detection of MCF-7†cells. Optical Materials, 2019, 88, 147-154.	3.6	4
38	In situ electrochemical reduction assisted assembly of a graphene-gold nanoparticles@polyoxometalate nanocomposite film and its high response current for detection of hydrogen peroxide. Electrochimica Acta, 2019, 300, 380-388.	5.2	38
39	A simple method for synthesis of highly efficient flower-like SnO2 photocatalyst nanocomposites. Journal of Materials Science: Materials in Electronics, 2019, 30, 50-55.	2.2	14
40	Development of a novel fluorescence ratiometric glucose sensor based on carbon dots and a potential fluorophore <i>m</i> -dihydroxybenzene. Analytical Methods, 2018, 10, 5380-5386.	2.7	13
41	S,N-Co-doped carbon nanoparticles with high quantum yield for metal ion detection, IMP logic gates and bioimaging applications. New Journal of Chemistry, 2018, 42, 20180-20189.	2.8	9
42	A novel highly fluorescent S,ÂN, O co-doped carbon dots for biosensing and bioimaging of copper ions in live cells. RSC Advances, 2018, 8, 42246-42252.	3.6	18
43	Determination of Lysozyme by Thiol-Terminated Aptamer-Based Surface Plasmon Resonance. Analytical Letters, 2017, 50, 682-689.	1.8	11
44	Room temperature phosphorescence of five PAHs in a synergistic mesoporous silica nanoparticle-deoxycholate substrate. Spectrochimica Acta - Part A: Molecular and Biomolecular Spectroscopy, 2017, 179, 233-241.	3.9	5
45	A highly selective and sensitive fluorescence sensor for the detection of apigenin based on nitrogen doped carbon dots and its application in cell imaging. Analytical Methods, 2017, 9, 6379-6385.	2.7	6
46	A rapid and highâ€ŧhroughput method for the determination of serum uric acid based on microarray technology and nanomaterial. Luminescence, 2017, 32, 730-734.	2.9	3
47	The Influence of Fluorination on Nano-Scale Phase Separation and Photovoltaic Performance of Small Molecular/PC71BM Blends. Nanomaterials, 2016, 6, 80.	4.1	4
48	Crystal structure of 4-(4-((3-bromophenyl)amino)-6-(<i>tert</i> -butyl)-3-(2-hydroxypropan-2-yl)cinnolin-8-yl)-2-methylbut-3-yn-2-ol, C ₂₆ H ₃₀ BrN ₃ O ₂ . Zeitschrift Fur Kristallographie - New Crystal Structures, 2016, 231, 1211-1213.	0.3	0
49	The effect of meta-substituted or para-substituted phenyl as side chains on the performance of polymer solar cells. Synthetic Metals, 2016, 220, 402-409.	3.9	3
50	A graphene oxide-based fluorescent aptasensor for alpha-fetoprotein detection. Analytical Methods, 2016, 8, 6131-6134.	2.7	16
51	The development of a novel chemiluminescent glucose sensor using hydrophilic Co ₃ O ₄ @SiO ₂ mesoporous nanoparticles. Analytical Methods, 2016, 8, 2923-2928.	2.7	5
52	Sensitive determination of kaempferol using carbon dots as a fluorescence probe. Talanta, 2015, 144, 390-397.	5.5	22
53	Development and cell imaging applications of a novel fluorescent probe for Cu ²⁺ . RSC Advances, 2015, 5, 69453-69457.	3.6	9
54	A label-free fluorescent sensor for Pb ²⁺ based on G-quadruplex and graphene oxide. Analytical Methods, 2014, 6, 8120-8123.	2.7	16

_		_	
- H E	NG		NC
	UVI.	1 6	IN U

#	Article	IF	CITATIONS
55	Room temperature phosphorescence of 9-bromophenanthrene, and the interaction with various metal ions. Spectrochimica Acta - Part A: Molecular and Biomolecular Spectroscopy, 2013, 102, 425-431.	3.9	4
56	Crystal structure of 1-methyl-5-(4-(1-methyl-1H-tetrazol-5-ylthio) butylthio)-1H-tetrazole, C8H14N8S2. Zeitschrift Fur Kristallographie - New Crystal Structures, 2013, 228, 11-12.	0.3	1
57			